Proc. Fifth Int. Conf. Clustering Aspects in Nucl. and Subnucl. Systems, Kyoto, 1988
J. Phys. Soc. Jpn. 58 (1989) Suppl. p. 693-698

Decay of Particle Unbound Fragmentation Products in ^{14}N+^{nat}Ag Reactions at 35 MeV/nucleon

T. Murakami, T.K. Nayak, W.G. Lynch, K. Swartz†, D.J. Fields††, C.K. Gelbke, Y.D. Kim, K. Kwiatkowski*, J. Pochodzalla**, M.B. Tsang, and F. Zhu

National Superconducting Cyclotron Laboratory and
Department of Physics and Astronomy,
Michigan State University,
East Lansing, MI 48824, USA
†Nuclear Physics Laboratory, University of Washington
Seattle, WA 98195, USA
††Physics Division, Lawrence Livermore National Laboratory,
Livermore, CA 94550, USA
*Department of Chemistry and Indiana University Cyclotron Facility,
Indiana University, Bloomington, IN 47405, USA
**Institut für Experimentalphysik, Universität Frankfurt,
D-600 Frankfurt, Fed. Rep. Germany

Correlations between coincident light particle (Z≦2) and heavy fragment (Z≧3) were measured for ^{14}N induced reactions on silver at E/A = 35 MeV/nucleon. Most relative energy spectra of p-shell nuclei exhibit several distinct structures which correspond to the location of excited states with J≧2. The measured relative populations deviate significantly from simple thermal model predictions. This finding strongly suggests the breakdown of the assumption of local thermal equilibrium at freezeout.

1. Introduction

When energetic hadronic-projectiles collide with relatively heavy-mass target nuclei, low energy intermediate mass fragments (Z>2) are emitted. This process is called nuclear fragmentation and anticipated to provide information concerning a highly excited nuclear system. In order to describe the fragmentation reaction several models have been proposed. Most of them, like the liquid-gas phase transition model, are based upon the assumption that the source of fragments can be approximated by a static, spatially homogeneous, and thermally equilibrated subsystem at a specific excitation energy and density.[1)] To apply such models one must be able to extract unique and consistent temperature from experimental data. Several attempts have been made to obtain temperature information from slope analyses of kinetic energy spectra of the emitted particles.[2)] Collective motion[3)] and/or the temporal evolution of the source,[4-6)] however, make the extraction of temperatures from the inclusive spectra rather unreliable.

Measurements of the relative populations of nuclear states, which are less sensitive to those problems, provide direct information about the internal excitation of emitted fragments and can be used to extract an "emission temperature", T, i.e. the temperature at freezeout, the time when the fragments leave the thermally equilibrated subsystem.[7-14)] In the simplest example, the ratio of populations, N_i/N_j, of two narrow states of a certain fragment is given approximately by

$$N_i/N_j = (2J_i+1)/(2J_j+1)\ \exp(-\Delta E/T), \qquad (1)$$

where $\Delta E = E_i - E_j$ and J_i and E_i are the spin and excitation energy of the i-th state of the fragment, respectively. If the sequential decay of higher lying states and much heavier particle unstable nuclei does not affect the populations N_i and N_j, the emission temperature T can be determined from the relative population of only two states in a given fragment. The influence of secondary processes such as sequential decay can be minimized by maximizing the energy difference ΔE between the excited states. Emission temperature has been measured for widely separated excited states in light ^{4}He, ^{5}Li, and ^{8}Be nuclei.[8,10,14] These measurements revealed that the relative populations of states have an amazingly small dependence on projectile energy; i.e., emission temperature was found to be T ≈ 4-5 MeV over the incident beam energy range of E/A = 35-94 MeV.[14] From measurements involving only two states, however, one cannot determine consistency of this approach. For a detailed test of this thermal assumption, the relative populations of many (>>2) states of a given fragment should be examined, requiring the study of heavier fragments which have many well resolved excited states.

In order to investigate the validity of the "local thermal equilibrium" assumption, we have developed a high resolution position sensitive heavy fragment hodoscope which enabled us to measure the populations of particle unstable states in p-shell nuclei emitted in the medium energy heavy-ion reactions.[15] In this report we present the first results obtained by using the new hodoscope.

2. Experimental Procedure

The experiment was performed by using 35 MeV/nucleon ^{14}N beam from the K500 cyclotron at the National Superconducting Cyclotron Laboratory of Michigan State University. A natural silver target of about 0.5 mg/cm² thickness was used for the measurement. The size of the beam spot on target was maintained within 3×3 mm². Light particles (Z≦2) and heavy fragments (Z≧3) were detected with a close-packed tetragonal array of 13 ΔE-ΔE-E telescopes. Nine of these telescopes were used to detect light particles and consisted individually of a 200 µm silicon surface barrier detector followed by a 5 mm Si(Li) detector, and a 10 cm-thick thin window NaI(Tl) detector. The other four telescopes were used to detect heavy fragments and consisted of a 75 µm silicon surface barrier detector followed by a 100 µm silicon surface barrier detector and a 5 mm Si(Li) detector. The energy resolution of these telescopes was about 150 keV. For each telescope position information was provided by a X-Y single resistive wire gas proportional counter positioned just in front of the telescope. Using this hodoscope we achieved an angular resolution of better than 0.2°. The solid angles of individual LP- and HF-telescopes were approximately 4.5 msr and 5.7 msr, respectively. The center of the hodoscope was set at laboratory angle of 38.4° which is significantly larger than the grazing angle (~6°). The angular separation between nearest neighbour telescopes was Δθ=8.0°; the one between farthest neighbour was 32.0°. The absolute normalization of the cross sections is accurate within 8%.

3. Experimental Results and Discussion

Yields of particle unstable nuclei are shown in Fig. 1 for the decays $^{14}N^* \rightarrow p + {}^{13}C$ and $^{10}B^* \rightarrow \alpha + {}^6Li$, as a function of the relative energy between light and heavy decay products. Background yield coming from uncorrelated coincident particles which do not arise from the decays of particle unstable $^{14}N^*$ or $^{10}B^*$ nuclei has been already subtracted for these spectra.[15] In these p-^{13}C and α-^{6}Li relative energy spectra several distinct structures are observed. These structures correspond to the particle unstable excited states with $J \geqq 2$; consistent with the spin degeneracy factors in eq. (1), the excited states with J=0 are not strongly populated.

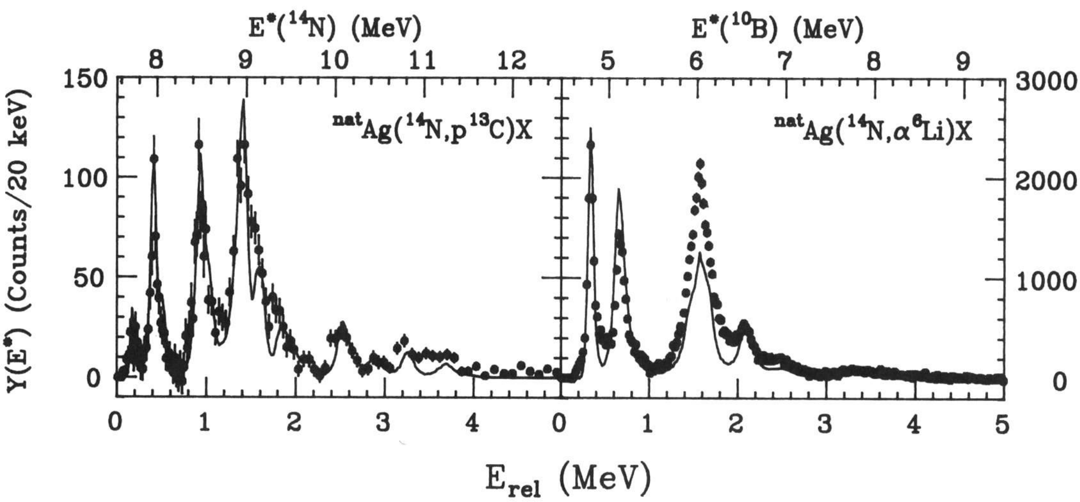

Fig. 1. The relative energy spectra for the particle unstable decays $^{14}N^* \rightarrow p + {}^{13}C$ and $^{10}B^* \rightarrow \alpha + {}^{6}Li$ measured in ^{14}N induced reactions on Ag at E/A=35 MeV/nucleon. The curves are explained in text.

The measured yield, Y(E*), for particle unbound nuclei at a measured excitation energy E* can be related to the decay spectrum, dn(E)/dE, of the particle unbound nucleus in its rest frame by the equation

$$Y(E^*) = \int \varepsilon(E^*,E) \frac{dn(E)}{dE} dE, \qquad (2)$$

where $\varepsilon(E^*,E)$ is the efficiency of the hodoscope for the detection of the particle unbound nucleus with actual excitation energy E. The efficiency function is affected by multiple scattering and energy loss in the target, resolution and geometry of the detector elements of hodoscope, the size of the beam spot on the target, the laboratory energy spectra and angular distributions of the particle unstable primary fragment, and any angular anisotropies in decay distribution of the primary fragment in its rest frame. This efficiency function was calculated using the actual conditions which prevailed during the experiment. The laboratory energy spectrum and angular distribution for such primary particle unstable nucleus was assumed to be the same as that measured for the same nucleus at its particle stable states. The decay distribution of the primary fragment in its rest frame was assumed to be isotropic.

Assuming the excitation energy spectrum dn(E)/dE for thermally emitted nuclei is given by

$$\frac{dn(E)}{dE} \propto \exp(-E/T) \sum_i \left[\frac{(2J_i+1)\ \Gamma_i/2\pi}{(E-E_i)^2 + \Gamma_i^2/4} \times \frac{\Gamma_{c,i}}{\Gamma_i} \right] \qquad (3)$$

where $\Gamma_{c,i}/\Gamma_i$ and Γ_i denote the compiled branching ratio for the decay into channel c' and the compiled total width, respectively, the experimental yield $Y(E^*)$ can be calculated via eq. (2). Calculations for the emission temperature T = 5 MeV are indicated by the solid curves in Fig. 1. Here we include 26 and 10 known particle unstable excited states in ^{14}N and ^{10}B, respectively. Spectroscopic information is obtained from Ref. 16. Consistent with previous observations, the general trend of the spectrum for the decay of particle unbound ^{14}N is well reproduced with a temperature of 4-5 MeV. It should be noted that the line shape of resonances is well reproduced by the calculation without adjusting the intrinsic resonance widths. Discrepancies between the calculated and measured ^{14}N decay spectra around E* = 9.1 and 9.3 MeV can be attributed to the decay of the 12.922 MeV 4^+ excited state in ^{14}N into the p + ^{13}C(3.854 MeV) and p + ^{13}C(3.685 MeV) channels, which we did not include into our calculations because the relevant decay branching ratios to these channels are not well known. In contrast, the decay spectrum for $^{10}B^* \rightarrow \alpha + {}^6Li$ shows a significant deviation from the theoretical prediction at an excitation energy of about 6 MeV. This structure corresponds to the unresolved excitation of the 2^+, E* = 5.92 MeV; 4^+, E* = 6.03 MeV and 3^-, E* = 6.13 MeV excited states of ^{10}B. This discrepancy cannot be removed by choosing another positive value of emission temperature. Similar discrepancies have also been observed in the p-^{10}B and p-^{11}C relative energy spectra.

In order to make a quantitative discussion of this discrepancy we have fitted the experimental decay spectra for $^{10}B^* \rightarrow \alpha + {}^6Li$ and $^{10}B^* \rightarrow p + {}^9Be$ by adjusting the population probability of the i-th state n_i in the equation

$$\frac{dn(E)}{dE} \propto \sum_i n_i \left[\frac{(2J_i+1)\,\Gamma_i/2\pi}{(E-E_i)^2 + \Gamma_i^2/4} \times \frac{\Gamma_{c,i}}{\Gamma_i}\right]. \qquad (4)$$

Since we could not individually resolve all states in the relative energy

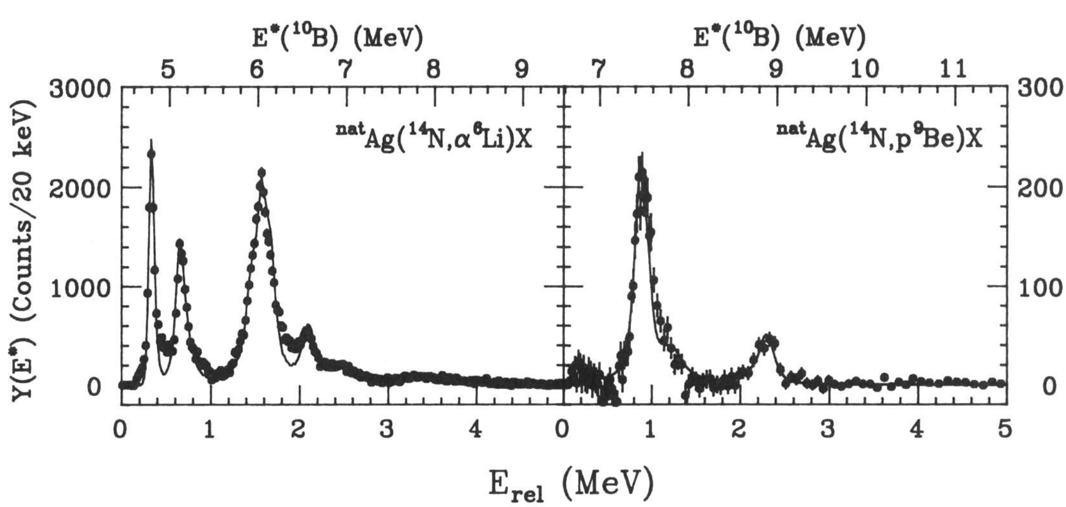

Fig. 2. The relative energy spectra for the particle unstable decays $^{10}B^* \rightarrow {}^6Li + \alpha$ and $\rightarrow {}^9Be + p$ measured in ^{14}N induced reactions on Ag at E/A= 35 MeV/nucleon. The curves are results of fitting explained in text.

spectra we have grouped unresolved excited states into several groups. Group 1, 2, 3, 4, 5, 6, and 7 correspond to the 4.774, (5.110, 5.164, 5.180), (5.920, 6.025, 6.127), 6.561, (7.430, 7.467, 7.479, 7.561), (7.67, 7.819, 8.07), and (8.889, 8.895) MeV excited states of ^{10}B, respectively. Within each group we have assumed that the population probabilities are identical. Results of fitting are shown in Fig. 2 together with experimental relative energy spectra. Good overall agreement with the experimental spectra is obtained. Figure 3 shows resultant population probabilities for each group of excited states as a function of excitation energy. Here the spin-degeneracy-factor weighted sum of the population probabilities for the particle stable states was normalized to one. The error bars reflected primarily the systematic errors of background subtraction. If local thermal equilibrium is achieved and secondary processes such as sequential decay are small the population probabilities n_i should fall off exponentially as a function of excitation energy, i.e., $n_i \propto \exp(-E_i/T)$. Since the data points in Fig. 3 are plotted in a logarithmic scale one would expect that they drop down along a straight line. As can be seen in the figure, however, the data points deviate significantly from this trend.

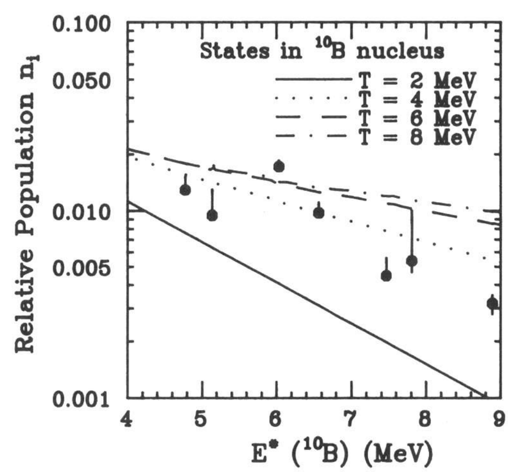

Fig. 3. Measured population probability n_i for ^{10}B as a function of excitation energy. The curves are explained in text.

It is important to know whether sequential feeding from heavier particle unstable nuclei can account for these deviations. We have performed detailed calculations in which the excited states of fragments A≦20 are populated thermally and allowed to decay statistically[17)] or if possible according to the available information concerning the branching ratios of those excited states. The results of calculations for emission temperature T=2, 4, 6 and 8 MeV are superimposed on the experimental data in Fig. 3. Clearly none of these calculations can reproduce the measured population. Inclusion in the calculation of high-lying continuum states up to E* = 5×A MeV does not improve this situation. This suggests that sequential feeding from heavier particle unstable nuclei is not responsible for the observed discrepancy.

We also examined the angular distributions for the α-decay of the particle unbound states in the center of mass frame of the excited ^{10}B. These decays were originally assumed to be isotropic. In fact α-decay of the states in group 1 and 2 occurs preferably in the reaction plane determined by the primary fragment and the beam axis. These anisotropies in the decay distributions change the detection efficiency about 10-15 %, but the magnitude of the change is too small to account the discrepancy between the experimental and theoretical populations. The existence of the anisotropy itself causes some difficulties for present thermal models for complex particle emission. Further works are clearly needed to solve these puzzles.

4. Summary

We investigated the relative population of particle unbound fragmentation products (7≦A≦16) for ^{14}N induced reactions on silver at E/A = 35 MeV. Experimental relative energy spectra indicated that most p-shell nuclei are frequently emitted at their particle unstable excited states with J≧2. The populations of these states differ significantly from simple thermal model predictions. Although the origin of this discrepancy is presently not completely understood, these results suggest that local thermal equilibrium is not achieved at freezeout.

Acknowledgments

This work was supported by the U.S. National Science Foundation under Grant No. PHY 86-11210 and by the U.S. Department of Energy under Contract No. DE-AC02-81ER-40007. One of authors (W.G.L.) acknowledges the receipt of the U.S. Presidential Young Investigator Award. Another of authors (J.P.) acknowledges the receipt of a fellowship from the Deutsche Forschungsgemeinschaft (W. Germany).

References

1) W. G. Lynch: Ann. Rev. Nucl. Part. Sci. **37**(1987)493.
2) G. D. Westfall et al.: Phys. Lett. **116B**(1982)118.
3) P. J. Siemens and J. O. Rasmussen: Phys. Rev. Lett. **42**(1979)880.
4) W. A. Friedman and W. G. Lynch: Phys. Rev. **C28**(1983)16.
5) D. J. Fields et al.: Phys. Rev. **C30**(1984)1912.
6) H. Stöcker et al.: Z. Phys. **A303**(1981)259.
7) D. J. Morrissey et al.: Phys. Lett. **148B**(1984)423; Phys. Rev. **C32**(1985)877.
8) J. Pochodzalla et al.: Phys. Rev. Lett. **55**(1985)177; Phys. Lett. **161B**(1985)275; Phys. Rev. **C35**(1987)1695.
9) D. J. Morrissey et al.: Phys. Rev. **C34**(1986)761.
10) C. B. Chitwood et al.: Phys. Lett. **172B**(1986)27.
11) A. Kyanowski et al.: Phys. Lett. **181B**(1986)43.
12) H. M. Xu et al.: Phys. Lett. **182B**(1986)155.
13) C. Bloch et al.: Phys. Rev. **C36**(1987)203.
14) Z. Chen et al.: Phys. Rev. **C36**(1987)2297.
15) T. Murakami et al.: to be published.
16) F. Ajzenberg-Selove: Nucl. Phys. **A413**(1984)1; Nucl. Phys. **A449**(1986)1.
17) D. J. Fields et al.: Phys. Lett. **187B**(1987)257.